Transcriptomic and metabolomic analysis of autumn leaf color change in *Fraxinus angustifolia*

Yanlong Wang [Equal first author, 1] , **Jinpeng Zhen** [Equal first author, 2] , **Xiaoyu Che** [1] , **Kang Zhang** [2] , **Guowei Zhang** [3] , **Huijuan Yang** [1] , **Jing Wen** [1] , **Jinxin Wang** [1] , **Jiming Wang** [1, 4] , **Bo He** [5] , **Ailong Yu** [6] , **Yanhui Li** [Corresp., 1] , **Zhigang Wang** [Corresp. 1]

[1] College of Landscape Architecture and Tourism, Hebei Agricultural University, Baoding, China

[2] Hebei Key Laboratory of Plant Physiology and Molecular Pathology, Hebei Bioinformatics Utilization and Technological Innovation Center for Agricultural Microbes, Hebei Agricultural University, Baoding, China

[3] Hongyashan State-owned Forest Farm in Hebei province, Baoding, China

[4] College of Grammar, Hebei Normal University of Science and Technology, Qinhuangdao, China

[5] Green Building Development Center of Baoding, Baoding, China

[6] Flower and wood Technical Service Center of Hengshui, Hengshui, China

Corresponding Authors: Yanhui Li, Zhigang Wang
Email address: yanhuili01@163.com, wzhg1956@163.com

Fraxinus angustifolia is a type of street tree and shade tree with ornamental value. It has a beautiful shape and yellow or reddish purple autumn leaves, but its leaf color formation mechanism and molecular regulation network need to be studied. In this study, we integrated the metabolomes and transcriptomes of stage 1 (green leaf) and stage 2 (red-purple leaf) leaves at two different developmental stages to screen differential candidate genes and metabolites related to leaf color variation. The results of stage 1 and stage 2 transcriptome analysis showed that a total of 5827 genes were differentially expressed, including 2249 upregulated genes and 3578 downregulated genes. Through functional enrichment analysis of differentially expressed genes, we found that they were involved in flavonoid biosynthesis, phenylpropanoid biosynthesis, pigment metabolism, carotene metabolism, terpenoid biosynthesis, secondary metabolite biosynthesis, pigment accumulation, and other biological processes. By measuring the metabolites of *Fraxinus angustifolia* leaves, we found the metabolites closely related to the differentially expressed genes in two different periods of *Fraxinus angustifolia*, among which flavonoid compounds were the main differential metabolites. Through transcriptome and metabolomics data association analysis, we screened nine differentially expressed genes related to anthocyanins. Transcriptome and qRT-PCR results showed that these nine genes showed significant expression differences in different stages of the sample, and we speculate that they are likely to be the main regulatory factors in the molecular mechanism of leaf coloration. This is the first time that we have analyzed the transcriptome combination metabolome in the process of leaf coloration of *Fraxinus angustifolia*, which has important

guiding significance for directional breeding of colored-leaf *Fraxinus* species and will also give new insights for enriching the landscape.

1 **Transcriptomic and metabolomic analysis of autumn leaf color change in**

2 *Fraxinus angustifolia*

4 Yanlong Wang[1,#], Jinpeng Zhen[2,#], Xiaoyu Che[1], Kang Zhang[2], Guowei Zhang[3], Huijuan Yang[1], Jing Wen[1],

5 Jinxin Wang[1], Jiming Wang[1,6], Bo He[4], Ailong Yu[5], Yanhui Li[1,*], Zhigang Wang[1,*]

6 1 College of Landscape Architecture and Tourism, Hebei Agricultural University, Baoding, 071000, China

7 2 Hebei Key Laboratory of Plant Physiology and Molecular Pathology, Hebei Bioinformatics Utilization and

8 Technological Innovation Center for Agricultural Microbes, Hebei Agricultural University, Baoding, 071000,

9 China

10 3 Hongyashan State-owned Forest Farm in Hebei province, Baoding, 071000, China

11 4 Green Building Development Center of Baoding, Baoding, 071000, China

12 5 Flower and wood Technical Service Center of Hengshui, Hengshui, 053000, China

13 6 College of Grammar, Hebei Normal University of Science and Technology, Qinhuangdao, 066000, China

15 # These authors contributed equally to this work

17 * Corresponding authors:

18 Yanhui Li

19 E-mail: yanhuili01@163.com

21 Zhigang Wang

22 E-mail: wzhg1956@163.com

24 **Abstract**

25 *Fraxinus angustifolia* is a type of street tree and shade tree with ornamental value. It has a beautiful

26 shape and yellow or reddish-purple autumn leaves, but its leaf color formation mechanism and

27 molecular regulation network need to be studied. In this study, we integrated the metabolomes and

28 transcriptomes of stage 1 (green leaf) and stage 2 (red-purple leaf) leaves at two different

29 developmental stages to screen differential candidate genes and metabolites related to leaf color

30 variation. The results of stage 1 and stage 2 transcriptome analysis showed that a total of 5827

31 genes were differentially expressed, including 2249 upregulated genes and 3578 downregulated

32 genes. Through functional enrichment analysis of differentially expressed genes, we found that

33 they were involved in flavonoid biosynthesis, phenylpropanoid biosynthesis, pigment metabolism,

34 carotene metabolism, terpenoid biosynthesis, secondary metabolite biosynthesis, pigment

35 accumulation, and other biological processes. By measuring the metabolites of *Fraxinus*

36 *angustifolia* leaves, we found the metabolites closely related to the differentially expressed genes

37 in two different periods of *Fraxinus angustifolia*, among which flavonoid compounds were the

38 main differential metabolites. Through transcriptome and metabolomics data association analysis,

39 we screened nine differentially expressed genes related to anthocyanins. Transcriptome and qRT-

40 PCR results showed that these nine genes showed significant expression differences in different

41 stages of the sample, and we speculate that they are likely to be the main regulatory factors in the

42 molecular mechanism of leaf coloration. This is the first time that we have analyzed the

43 transcriptome combination metabolome in the process of leaf coloration of *Fraxinus angustifolia*,

44 which has important guiding significance for directional breeding of colored-leaf *Fraxinus* species

45 and will also give new insights for enriching the landscape.

46

47 **Keywords:** *Fraxinus angustifolia*; transcriptomes; metabolomes; anthocyanin; gene expression

48

1. Introduction

49

50 Colored-leaf plants refer to plants whose leaves are stable, non-green, and of obvious ornamental

51 value in certain seasons or throughout the year (Wang et al. 2016). As important as flower color,

52 leaf color is a significant ornamental trait of plants. The pigment content in colored-leaf plants is

53 affected by specific factors, especially the ratio of carotenoids or anthocyanins to chlorophyll,

54 which leads to red or yellow leaves (Cheng et al. 2015). Developed countries have been engaged

55 in the cultivation and application of colorful plants for more than one 100 years. In the United

56 States, Canada, and other countries, the planting area of colored-leaf trees can reach more than

57 30% that of all trees (Özbayram & Çiçek 2018).

58   There are three main categories of pigments: chlorophyll, mainly chlorophyll a and

59 chlorophyll b; carotenoids, mainly carotenoids and lutein; and three flavonoid pigments, also

60 known as anthocyanins (Tanaka et al. 2008). Different pigments appear in different colors;

61 ordinary leaves contain more chlorophyll than carotenoids, so the leaves are always green (Tanaka

62 et al. 2008). Studies have shown that a combination of flavonoids, anthocyanins, and carotenoids

63 can increase leaf color diversity (Luiza Koop et al. 2022). *Ginkgo biloba* L, *Pseudolarix amabilis,*

64 and other leaves contain more carotenoids and appear yellow; anthocyanins, such as in *Acer*

65 *palmatum* Thunb and *Acer buergerianum* Miq, appear red when their content increases.

66 *Amaranthus tricolor* has leaves from purple to bright red, which is also due to cell senescence and

67 chlorophyll reduction, so that the color of anthocyanins shows (Sharma et al. 2021). Carotenoids

68 and anthocyanins also play an important role in the photoprotection of photosystems, which help

69 plants adapt to the environment and maintain the proper functioning of their internal mechanisms

70 during leaf senescence (Das et al. 2011; Hashimoto et al. 2016).

71   The massive accumulation of anthocyanins is the basic material for the reddening of colorful

72 plant leaves (Zhang et al. 2019). Many studies have shown that the change in leaf color

73 anthocyanin content in colored-leaf plants is the result of interaction of environmental factors and

74 internal factors (Santos-Buelga et al. 2014). Temperature drop and a shortened photoperiod in

75 autumn and winter often trigger genetic signals for chlorophyll decomposition (Song et al. 2013).

76 With the decomposition of amino acids, proteins, and other substances in leaves and migration of

77 nutrients in leaves, the chlorophyll content gradually decreases with time, while the anthocyanin

78 content gradually increases, making the leaves red (Li et al. 2018). At the same time, the synthesis

79 and accumulation of anthocyanins is closely related to sugar, protein, chlorophyll, carotenoids,

80 and other substances in plants, and is affected by natural environmental factors such as light time,

81 light intensity, and temperature changes (Zhang et al. 2016).

82 Anthocyanins are produced by flavonoid compounds through the shikimic acid synthesis

83 pathway, synthesized in the cytoplasm, and eventually stored in plant cell vacuoles (Mishio et al.

84 2015). This synthetic pathway is an important branch of the plant flavonoid biosynthesis pathway,

85 and it is also one of the most important pathways for the synthesis of plant secondary metabolites

86 (Zhao et al. 2022). The precursors of anthocyanin synthesis are malonic acid monophthalide-CoA

87 and 4-hydroxybenzoic acid-CoA, and the final product anthocyanin is produced by a series of key

88 enzymes, such as chalcone synthase (CHS), chaleone isomerase (CHI), dihydroflavonol reductase

89 (DFR), and glycosyltransferase (GT) (Tanaka et al. 2008). Anthocyanin metabolism is affected by

90 key enzyme genes and transcription factors (Tanaka et al. 2008). Key enzyme genes directly

91 encode the key enzymes required for anthocyanin synthesis (Zhou et al. 2017).

92 *Fraxinus angustifolia* is an important afforestation tree species in northern China (Sarfraz et

93 al. 2017). *Fraxinus angustifolia* has an upright body, straight trunk, and luxuriant branches and

94 leaves, and it is an excellent street tree and shade tree, as autumn-colored tree species have become

95 favored for good landscape effects in recent years (Manzanera & Martinez-Chacon 2007;

96 Özbayram & Çiçek 2018). However, research on the change of leaf color has been limited. In this

97 study, transcriptome and metabolome sequencing analysis was performed on the leaves of two

98 critical periods of *Fraxinus angustifolia* to explore the genes related to the leaf coloration of

99 *Fraxinus angustifolia* and their regulatory networks, and then to screen out the genes that may be

100 related to the metabolic process of anthocyanins and leaf color expression. The results of this study

101 provide a theoretical basis for elucidating the mechanism of leaf color formation, and they reveal

102 the role and molecular mechanism of anthocyanins in the leaves of *Fraxinus angustifolia*. This has

103 important guiding significance for directional cultivation of colored-leaf *Fraxinus* varieties and

104 will also provide important technical support for the study of molecular regulation mechanisms of

105 colored-leaf traits in woody plants.

106

107 **2. Materials and Methods**

108 **2.1 Plant Materials**

109 The leaves of 6-year-old *Fraxinus angustifolia* were collected from Baoding, Hebei Province in

110 October. Then, the leaves of *Fraxinus angustifolia* were quickly frozen in liquid nitrogen bottles,

111 and then transferred to an ultra-low temperature refrigerator for cryopreservation for RNA and

112 metabolite extraction.

113 **2.2 RNA Extraction, Library Construction, and Sequencing**

114 Total RNA was extracted from the sample using TRIzol (Invitrogen, Massachusetts, USA) and

115 purified using a RNeasy column (Qiagen, Dusseldorf, Germany). mRNAs were enriched with

116 Oligo(dT) beads After total RNA extraction. Enriched mRNA fragments were split into short

117 fragments and reverse transcribed into cDNA. The cDNA fragment was then purified using the

118 QiaQuick PCR extraction kit (Qiagen, Venlo, the Netherlands), the ends were repaired, poly(A)

119 was added, and it was connected to the Illumina sequencing adapter. The ligation products were

120 size selected by agarose gel electrophoresis. After PCR amplification and quality inspection, DNA

121 fragments were sequenced using Illumina HiSeq^{TM} 4000.

122 **2.3 Transcriptome Low Quality Data Filtering**

123 FastQC (Brown et al. 2017) software was used to filter the data. The parameters were as follows:

124 a) delete the read containing the adapter; b) remove reads containing more than 10% unknown

125 nucleotides (N); c) remove low quality reads containing more than 50% low quality (q value≤20)

126 bases.

127 **2.4 Transcriptome Data Assembly and Integrity Assessment**

128 The obtained high-quality reads were assembled and annotated using Trinity software (Sewe et al.

129 2022). Trinity is a modular approach and software package that consists of three parts: Inchworm,

130 Chrysalis, and Butterfly. First, the Inchworm was read by the k-mer method to obtain a linear

131 contigs set. Next, Butterfly aggregated the related contigs corresponding to the unique part of the

132 alternatively spliced transcript or the accessory gene and then constructed a de Bruijn diagram for

133 each related contigs cluster. Finally, Butterfly analyzed the path taken to read and read the pairing

134 in the corresponding de Bruijn diagram, and it then output a linear sequence for each alternatively

135 spliced isoform and script obtained from the fallacy gene. At the same time, BUSCO software was

136 used to evaluate the integrity of the assembly results (Manni et al. 2021).

137 **2.5 Transcriptome Annotation and Differential Gene Analysis**

138 Firstly, the assembled Unigene sequences were compared to the Nr database, KEGG, COG/KOG,

139 and SwissProt by blastx. Based on Nr annotation information, we used Blast2GO software to

140 obtain GO function annotation (Conesa & Gotz 2008). At the same time, the Pfam_Scan program

141 was used to compare with the Pfam database to obtain annotation information related to protein

142 structure. The HMMER program was compared with the SMART database to obtain the

143 annotation information of the protein domain. The PlantTFDB database was compared by

144 hmmscan to obtain transcription factor annotation information (Jin et al. 2017). DESeq2 software

145 was used to analyze differentially expressed genes (DEGs) between groups (Love et al. 2014). The

146 analysis was divided into three parts: a) standardization of readcount; b) calculation of the

147 probability of hypothesis testing (P-value) based on the model; and c) multiple hypothesis test

148 correction to obtain the FDR value (false discovery rate). Based on the results of differential

149 analysis, the genes of FDR were screened as significantly differential genes.

150 **2.6 Gene Function Enrichment Analysis**

151 Gene ontology is an internationally standardized gene function classification system that fully

152 describes the characteristics of genes and their products in organisms. The differential genes are

153 mapped to GO database. AgriGO v2.0 custom tools KOBAS-i was employed to GO and KEGG

154 enrichment analysis, respectively (Tian et al. 2017, Bu et al. 2021).

155 **2.7 Metabolite Extraction**

156 The biomaterial samples, preserved at ultra-low temperatures, were taken out and vacuum freeze-

157 dried. Samples were ground by a grinding machine at 30 Hz for 1.5 min, and 100 mg of powder

158 was weighed. The powder was extracted overnight at 4℃ with 70% methanol 1.0 ml containing

159 0.1 mg/l lidocaine as an internal standard, and vortexed three times to make the extraction more

160 sufficient. After extraction, it was centrifuged at 10,000 g for 10 min, the supernatant was

161 aspirated, and the sample was filtered through a microporous membrane (0.22 μm pore size) and

162 stored in a sample bottle for subsequent LC-MS analysis. A quality control sample (QC) was

163 prepared by mixing sample extracts to analyze the repeatability of samples under the same

164 treatment method. Usually, a QC sample was inserted every 10 samples to investigate the

165 repeatability of the analysis process.

166 **2.8 Detection of Metabolites**

167 Conditions for UPLC analysis were as follows: An analytical column Mobile phase: ultrapure

168 water (0.04% acetic acid added), acetonitrile (0.04% acetic acid added); elution gradient: 0 min

169 water/acetonitrile (95:5V/V), 11.0 min 5:95V/V, 12.0 min 5:95V/V, 12.1 min 95:5V/V, and 15.0

170 min 95:5V/V. Waters ACQUITY UPLC HSS T3 C18 1.8 There was a 0.4 ml/min flow. 40 °C for

171 the column; a 2 l input volume. ESI-QTRAP-MS was used to evaluate the separated samples.

172 The primary settings for the linear ion trap and triple quadrupole in the API 6500 QTRAP

173 LC/MS/MS system were as follows: collision-activated dissociation (CD) parameter setting of

174 high, electrospray ionization (ESI) temperature of 550 °C, mass spectrometry voltage of 5500 V,

175 curtain gas (CUR) of 25 psi. Each ion pair is scanned in a triple quadrupole (QQQ) using an

176 optimum declustering potential (DP) and collision energy (CE). The software Analyst 1.6.1 was

177 used to process the data.

178 **2.9 Metabolomics Data Analysis**

179 Peaks were manually examined for signal/noise (s/n) > 10, and internal Perl software was used to

180 eliminate duplicate signals brought on by various isotopes, in-source fragmentation, K^+, Na^+, and

181 $NH4^+$ adduct, and dimerization. This resulted in a matrix with fewer skewed and redundant data.

182 Accurate m/z for each Q1 was collected to make it easier to identify and annotate metabolites. To

183 provide a summary of the metabolite profiles of all samples, total ion chromatograms (TICs) and

184 extracted ion chromatograms (EICs or XICs) of QC samples were exported. Each chromatographic

185 peak's area was determined. Peak alignment was done between the several samples using the

186 spectral pattern and retention time. Metabolites were identified by searching internal database and

187 public databases (MassBank, KNApSAcK, HMDB, MoToDB, and METLIN) and comparing the

188 m/z values, the RT, and the fragmentation patterns with the standards.

189 Statistical analysis (PCA analysis and OPLS-DA analysis) used the VIP value and P value to

190 screen differential metabolites. Through inter-group difference analysis, differentially expressed

191 genes were obtained from transcriptome data, differentially expressed metabolites were obtained

192 from metabolomics data, and KEGG enrichment analysis of each group was performed. The

193 correlation analysis of common KEGG pathways was carried out for the differential genes and

194 metabolites between groups.

195 **2. 10 Transcriptome Metabolome O2PLS Model Analysis**

196 Based on all transcriptome and all metabolome data, we performed O2PLS analysis using the

197 OmicsPLS package (Bouhaddani et al. 2018). The O2PLS model is suitable for association

198 analysis of two omics data and can be used for bidirectional modeling and prediction in two data

199 matrices. Through calculation, the O2PLS model decomposes the data of each omics into three

200 parts, namely, the joint part (A part, that is strongly related to another group), the orthogonal part

201 (parts that affect only one group of data and have no effect on another omics data), and the noise

202 part (parts that have no effect on both sets of data). The degree to which each component explains

203 the total variation is expressed as R2, and Higher values represent better model explanatory power.

204 Overfitting and underfitting of models reduce R2.

205 **2.11 Correlation Coefficient Analysis**

206 The Pearson correlation coefficient can be used to measure the relationship between two variables,

207 representing the strength of co-variation between two variables, ranging from -1 to +1. The

208 Pearson coefficient of the expression of all differential genes (the union of differential genes

209 between each comparison group) and the abundance of all differential metabolites (the union of

210 differential metabolites between each comparison group) was calculated to evaluate the correlation

211   between genes and metabolites.

212

3. Results

3.1 Transcriptome Data filtering and Assembly Analysis

To explore the mechanism of leaf color change in *Fraxinus angustifolia*, we sequenced the *de novo* transcriptomes of *Fraxinus angustifolia* leaves at two different growth stages. Based on the transcriptome data, after quality control, the clean reads of six samples were 5,766,222,300– 10,874,368,200, the Q30 base percentage was 93.73–95.20%, and the GC content was 44.98– 45.44% (Table S1). The overall sequencing filtering quality was good and could be used for subsequent transcriptome analysis. Through transcriptome assembly, we obtained 74,430 Unigenes with a length ranging from 201 bp to 16,676 bp, with an average length of 863 bp (Fig. 1B). According to the distribution of Unigene with different lengths after assembly, the length of 0–500 bp accounted for about 60% of the total. In the splicing results, the N50 length was 1458 bp. The integrity of the assembled transcripts was evaluated by BUSCO (Fig. S1), and the integrity was 75.56%, indicating that the integrity of the transcriptome data was high.

3.2 Functional Annotation Analysis of Unigenes

To explore the gene function of the unigenes, we used four databases (Nr, KEGG, KOG, SwissProt) to annotate the obtained Unigenes (Fig.1C). Finally, 44,746 genes with annotation information were obtained, and 29,684 Unigenes were not annotated, with an annotation ratio of 60.12%. Among them, 43,150 Unigenes were annotated in the Nr database, 39,999 Unigenes were annotated in the KEGG database, 24,903 Unigenes were annotated in the KOG database, and 30,315 Unigenes were annotated in the Swissprot database. Among them, 20,659 genes had annotation information in four databases.

3.3 Gene Differential Expression Analysis of Transcriptome Data

In order to ensure the accuracy of subsequent analysis, we first corrected the sequencing depth, and then corrected the length of the gene or transcript to obtain the RPKM value of the gene, and then performed the subsequent analysis. Based on the RPKM value of each gene, the expression

238 distribution was calculated. As can be seen from the distribution, gene expression is more uniform

239 between different samples, meaning that these results can be used for subsequent differential gene

240 analysis (Fig. 2A). Principal component analysis (PCA) and pearson correlation coefficient

241 analysis clustered the samples based on the expression level. Through PCA analysis between these

242 samples, results showed that three biological replicates of samples from different periods were

243 distributed in the same quadrant (Fig. 2B). Pearson correlation coefficient analysis showed the

244 correlation of each two samples was above 0.85 (Fig. S2), indicating that the sample repeatability

245 was good. A total of 5827 DEGs were found between stage 1 (green leaf stage) and stage 2 (red

246 purple leaf stage), of which 2249 were upregulated and 3578 were downregulated (Figure 2C and

247 2D).

248 **3.4 Functional Analysis of Differential Genes**

249 To elucidate the function of differentially expressed genes in leaf color change of *Fraxinus*

250 *angustifolia*, GO enrichment analysis of differentially expressed genes was performed. Based on

251 the results of GO functional enrichment analysis, the differentially expressed genes in stage 1

252 (green leaf stage) and stage 2 (red purple leaf stage) were mainly enriched in flavonoid anabolism,

253 programmed cell death, phenylpropanoid anabolism, chloroplast quinone metabolism, pigment

254 metabolism, carotene metabolism, polysaccharide metabolism, terpenoid anabolism, jasmonic

255 acid metabolism, fatty acid anabolism, photosynthesis, secondary metabolite biosynthesis,

256 pigment accumulation, and other biological processes (Fig. 3A). In the molecular function

257 classification, the differentially expressed genes were significantly enriched in terms of

258 oxidoreductase activity, monooxygenase activity, hydrolase activity, transferase activity,

259 tetrapyrrole binding, nucleic acid binding transcription factor activity, carotenoid dioxygenase

260 activity, antioxidant activity, fatty acid synthase activity, galactosyltransferase activity, and iron

261 ion binding (Fig. 3B). In the classification of cell composition, GO terms were mainly enriched in

262 the thylakoid, chloroplasts, photosynthetic membranes, cell wall, peroxisome, photosystem, light-

263 harvesting complex, thylakoid membrane, etc (Fig. 3C).

264   Then, KEGG pathway enrichment analysis was performed with differentially expressed

265   genes to analyze the key enriched metabolic pathways in leaf color change of *Fraxinus*

266   *angustifolia*. Based on the results of KEGG metabolic pathway enrichment analysis, we found that

267   the differentially expressed genes between stage 1 (green leaf) and stage 2 (red-purple leaf) were

268   significantly enriched in metabolic pathways such as secondary metabolite biosynthesis,

269   phenylpropanoid biosynthesis, riboflavin metabolism, flavonoid biosynthesis, anthocyanin

270   biosynthesis, carotene biosynthesis, terpenoid biosynthesis, steroid biosynthesis, and thiamine

271   metabolism (Fig. 4). The functional enrichment analysis indicated that differentially expressed

272   genes played an important role in leaf color change of *Fraxinus angustifolia*.

273   **3.5 Analysis of Differential Metabolites in Leaves of *Fraxinus angustifolia* at Different Stages**

274   Leaves show different colors mainly due to internal pigment-related components and content. The

275   leaves of different periods of *Fraxinus angustifolia* have significant color differences in phenotype

276   (Fig. 1A). Through the determination of the metabolome, the leaves of *Fraxinus angustifolia* in

277   these two periods can be divided into two groups with significant differences according to PCA

278   analysis, based on the content of their internal metabolites (Fig. 5A). To further identify the

279   metabolites associated with leaf color difference, we used orthogonal partial least squares

280   discriminant analysis (OPLS-DA) to explore the differential metabolites between different colors.

281   Cross-validation and ranking validation showed that the OPLS-DA model of each comparison

282   group was meaningful (Fig. 5B). Then, we obtained the relevant load diagram by OPLS-DA

283   analysis (Fig. 5B and S3). The farther the metabolites from the origin in the OPLS-DA loading

284   plot, the greater their contribution to the separation of leaf color categories of *Fraxinus*

285   *angustifolia*. Organic acids, lipids, and flavonols are the main substances that cause differences in

286   the metabolome level of *Fraxinus angustifolia* at different stages, while flavonols are the main

287   factors that cause differences in leaf color at different stages.

288   Furthermore, according to the criteria for identifying differential metabolites (VIP>1, t-test

289   P-value<0.05), we identified a total of 118 compounds. Compared with stage 1 (green leaf stage)

290   and stage 2 (red purple leaf stage), with 40 kinds of material accumulation, there were 13 kinds of

291   flavonoid compounds, including 8 kinds of flavonols and 4 kinds of flavonoids (Fig. 5C).

292 Therefore, we speculate that flavonoid compounds may be the main factor causing the change of

293 leaf color of *Fraxinus angustifolia*.

294   Based on the metabolic pathway enrichment analysis of differential metabolites, we found

295 that the differential metabolites in stage 1 (green leaf stage) and stage 2 (red purple leaf stage)

296 were mainly enriched in secondary metabolite biosynthesis, aminoacyl-tRNA biosynthesis, 2-

297 oxocarboxylic acid metabolism, glucosinolate biosynthesis, carbapenem biosynthesis,

298 cyanoamino acid metabolism, phenylpropanoid biosynthesis, ubiquinone and other terpenoid

299 quinone biosynthesis, riboflavin metabolism, porphyrin and chlorophyll metabolism, fatty acid

300 biosynthesis, the TCA cycle, tryptophan metabolism, niacin and nicotinamide metabolism, and

301 other metabolic pathways (Fig. 5D). Based on the above results, we found that the pathways related

302 to anthocyanin synthesis were significantly enriched, which provided an important basis for

303 subsequent analysis.

304 **3.6 Association Analysis of DEGs and Metabolites Between the Green and Red-Purple Leaf**

305 **Stage**

306 To calculate the gene expression and metabolite abundance, we used pearson correlation

307 coefficient to evaluate the correlation between genes and metabolites in stage 1 and stage 2. Then,

308 we performed a loading plot analysis on the association between genes and metabolites to analyze

309 the contribution of each variable (metabolites, genes) to the differences between groups based on

310 the O2PLS model analysis. The loading value represents the explanatory power of the variables

311 (metabolites, genes) in each component (the contribution to the difference between groups), and

312 the positive or negative value of the loading value indicates a positive or negative correlation with

313 another group. The larger the absolute value of the load value, the stronger the correlation. By

314 comparing and analyzing the correlation between differential genes and metabolites in the two

315 periods, we found that they were located at both ends of the ordinate; that is, the absolute values

316 were very large (Figure 2), indicating that the data in this part were highly correlated, which

317 provided a reliable basis for further analysis. Through the analysis of the most relevant top 25

318 results in the association analysis results, we found that the metabolites in stage 1 (green leaf stage)

and stage 2 (red-purple leaf stage) were amino acids and their derivatives, sesquiterpenes, dihydroflavonols, flavonoids, flavonols, triterpenoids, vitamins, coumarins, phenolic acids, lignans, and organic acids, respectively. The genes associated with them were MYB transcription factors, DNA glycosylase superfamily proteins, NAC domain-containing proteins, etc. (Fig. 6A).

Through the network association analysis of genes or metabolites in important association positions, we screened out the key associated genes and metabolites, and focused on the analysis of the results of the top 250 (Figure 6B). The core metabolites were flavonols (Lmmp002334, Lmyp004444, Hmpp003242), alkaloids (pmp001275), free fatty acids (pmp001276), phenolic acids (mws0885, mws0183), flavonoids (Hmpp003270), amino acids and their derivatives (pme0193), and organic acids (mws0639). The genes related to them were various transcription factors (*MYB, NAC, bHLH, WRKY, TCP*, etc.) and various enzymes.

3.7 Screening of Anthocyanin Synthesis-Related Genes

Based on the above transcriptome and metabolomics data analysis results, we found that differential genes or substances were mainly concentrated in the anthocyanin synthesis pathway. Therefore, we analyzed the genes related to the anthocyanin synthesis pathway. Through the analysis of expression differences, we screened seven genes with higher expression levels in the red and purple leaf stage of the leaves of *Fraxinus angustifolia* (Figure 7A and 7B), which were *Unigene0029203*(*4CL3*), *Unigene0037675*(*PAL*), *Unigene0061770*(*DFRA*), *Unigene0009106*(*CHI*), *Unigene0010118*(*PAL*), *Unigene0037674*(*PALA*), and *Unigene0002804*(*CHI3*). The significant differential expression of these genes in two different periods may be closely related to the change of leaf color.

Anthocyanins are not stable in plant cells, and they are generally modified (methylation, acylation, glycosylation, etc.) to form more stable and richer anthocyanidin, which directly determine the color of plant tissues. We further analyzed the genes related to the anthocyanidin biosynthesis pathway in the transcriptome data and found that two Unigenes in the anthocyanidin biosynthesis pathway were upregulated at the red-purple leaf stage (Fig. 7C and 7D), one of which was *Bronze-1* (*BZ1, anthocyanidin 3-O-glucosyltransferase gene*) and the other gene was

346   *UGT79B1* (*anthocyanidin 3-O-glucoside 2'-O-xylosyltransferase gene*) (Fig. S4). These two genes

347   showed significant expression differences in different samples, indicating that they may play an

348   important role in leaf color change.

349

350   **4. Discussion**

351   Environmental changes can lead to changes in the color of plant leaves. Usually, changes in

352   external conditions such as temperature, light, humidity, stress environment, reproductive growth,

353   and other external conditions can induce plant leaves to produce corresponding signals, thereby

354   regulating the expression of leaf color change-related genes and the occurrence of related

355   physiological processes, so that leaves show different colors (Sork et al. 2010). Studying the

356   physiological and molecular regulation mechanism of leaf discoloration of color-leafed plants,

357   exploring the related genes involved in leaf color regulation, and clarifying their functions and

358   mechanisms will lay a solid theoretical foundation for enriching the landscape and provide

359   important theoretical guidance for the application and promotion of color-leafed tree species (Zhao

360   et al. 2020).

361   Pigments in plants mainly include chlorophyll, carotenoids, flavonoids, and anthocyanins

362   (Zhao et al. 2020). Red is mainly derived from the composition and content of flavonoids.

363   Flavonoids are mainly anthocyanins and belong to the more important secondary metabolites,

364   mainly cyanidin aglycone, delphinidin aglycone, pelargonidin aglycone, peoniflorin aglycone,

365   petunidin, and malvidin 6 anthocyanins derived from aglycone. When the anthocyanin content is

366   high, the leaves appear red (Kong et al. 2003). New red leaves of tree peony are due to increased

367   anthocyanin content and decreased chlorophyll and carotenoid content (Luo et al. 2017). The

368   anthocyanin content in young leaves of jatropha is 11 times the chlorophyll content, mostly in

369   epidermal cells, making leaves red (Ranjan et al. 2014). In this study, we performed transcriptome

370   analysis of the leaves of *Fraxinus angustifolia* and found that 5827 genes were differentially

371   expressed at two different developmental stages. GO enrichment analysis showed that the

372   differentially expressed genes in the three periods were significantly enriched in flavonoid

373 anabolism, phenylpropanoid anabolism, chlorophyll quinone metabolism, pigment metabolism,

374 carotene metabolism, polysaccharide metabolism, terpenoid anabolism, jasmonic acid

375 metabolism, fatty acid anabolism, photosynthesis, secondary metabolite biosynthesis, pigment

376 accumulation, and other terms, indicating that the differentially expressed genes enriched in these

377 terms may play an important role in leaf color change of *Fraxinus angustifolia*.

378 At the same time, KEGG metabolic pathway enrichment analysis showed that the differential

379 genes were significantly enriched in the phenylpropanoid biosynthesis pathway, which is

380 responsible for the anabolism of flavonoids, such as anthocyanins, flavonols, and flavanols (Liu et

381 al. 2021). In many plants, the flavonoid pathway exists in colored tissues and is the main cause of

382 color changes, such as *Tulipa gesneriana* (Guo et al. 2022), *Prunus persica*(Ravaglia et al. 2013),

383 etc. Through gene function annotation, it is valuable to understand the accumulation of

384 anthocyanins, and it is also important for further study of functional genes (Santos-Buelga et al.

385 2014; Belwal et al. 2020). In this study, KEGG enrichment analysis identified two important

386 pathways related to anthocyanin biosynthetic metabolism; the flavonoid biosynthesis pathway,

387 flavonoid and flavonol biosynthesis pathways, and anthocyanin metabolic pathways related to

388 anthocyanin substrate synthesis. Therefore, these genes may have a direct correlation with the

389 synthesis of anthocyanin in *Fraxinus angustifolia*.

390 Plant metabolomics enables qualitative and quantitative analysis of small molecule

391 metabolites and understanding of their synthesis and metabolic patterns (Schauer & Fernie 2006;

392 Wang & Kadarmideen 2020). At present, the results show that the study of plant metabolites is

393 important for the identification of metabolites, variety differentiation and molecular breeding

394 (Rizzato et al. 2017; Zhou et al. 2017). The formation of plant color is closely related to the

395 anabolism of flavonoids (Zhang et al. 2017). In the metabolomic analysis of flavonoids in white

396 and purple flowers of Phalaenopsis, 142 different flavonoid-related metabolites were identified,

397 proving that the major anthocyanin is a cyanide derivative (Meng et al. 2020). In this study, we

398 determined the metabolites of the leaves of *Fraxinus angustifolia*, and OPLS-DA analysis showed

399 that flavonols were the main factors for the difference of leaf color in different periods of *Fraxinus*

angustifolia, and 118 compounds were identified. It is speculated that flavonoid compounds may be the main factor causing leaf color changes. The metabolic pathway enrichment analysis of differential metabolites showed that the metabolic pathways related to anthocyanins synthesis were significantly enriched, which provided an important basis for downstream analysis.

It has been confirmed in plants that transcription factor families, such as MYB and bHLH, are essential for inducing anthocyanin biosynthesis pathways (Allan et al. 2008; Tanaka et al. 2008). For example, mutations in these regulatory genes usually lead to color changes in apple, *Actinidia chinensis* purple cauliflower (*Brassica oleracea* L.), *Dahlia pinnata,* and tomatoes (Butelli et al. 2008; Chiu et al. 2010; Ohno et al. 2011; Wang et al. 2019; Sun et al. 2021). We further performed correlation analysis of transcriptome and metabolome data, and we found that there were multiple common metabolic pathways in stage 1 (green leaf stage) and stage 2 (red-purple leaf stage). Based on the O2PLS model analysis, we found that the flavonoid compounds in the substances closely related to the genes in two different periods had a high proportion and were at the core association position of the metabolite network diagram. We found that flavonoid compounds are closely related to transcription factors, such as phenolic acids (mws0183, mws0885, mws1195, mws1200, and pmb2795), flavonoids (HJAP064, HJAP065, Hmpp003270, Xmyp005261, and Zmhp005139), and flavonols (Hmpp003242, Lmdp003808, Lmmp002334, Lmyp004444, and pmp001311). Association analysis results showed that more than 200 genes were closely related to these metabolites, among which transcription factors such as MYB, bHLH, and NAC were closely related to these metabolites. Therefore, these results indicated that transcription factors play an important role in the change of flavonoid compounds during the change of leaf color in autumn. In addition, we also screened nine differentially expressed genes related to anthocyanins. Transcriptome data and qRT-PCR results showed that these genes had significant expression differences in samples of different periods of *Fraxinus angustifolia*. We predicted that they were the key structural genes of anthocyanin biosynthesis and the main factors regulating leaf color changes, which provided an important basis for further analysis of the molecular regulation mechanism of leaf coloration of *Fraxinus angustifolia*.

427

428

Author contributions

Conceived and designed the experiments: Y. Li, K. Zhang, Z. Wang. Performed the experiments: Y. Wang, X. Che, J. Zhen, G. Zhang, H. Yang, J. Wen. Data analysis: Y. Wang, X. Che, J. Zhen, J. Wang, J. Wang, B. He, A. Yu. Wrote the paper: Y. Li, K. Zhang, Z. Wang.

Funding

This work was supported by Key project of Education Department of Hebei Province (ZD2022009), National Key Research and Development Project (2020YFD1000700), and Funding Program for Visiting Scholar Abroad (C20200334).

Data Availability

The RNA-seq datasets and transcript assembly data generated in this study are available in National Genomics Data Center (NGDC) databases, under Bioproject accession number PRJCA014072 that is publicly accessible at https://ngdc.cncb.ac.cn/.

Competing Interests

The authors declare no conflict of interest.

447 **Figure legends**

448 **Figure 1.** Statistical analysis of transcriptome data. (A) Leaf states at stage 1 and stage 2. (B)

449 Length distribution of Unigene in transcriptome assembly. (C) Venn diagram of Unigene

450 annotation in the Nr, KEGG, KOG, and SwissProt databases.

451

452 **Figure 2.** Expression analysis of Unigenes in stage 1 and stage 2. (A) Expression level analysis of

453 different biological replicates in stage 1 and stage 2. (B) Principal component analysis (PCA) of

454 expression datasets in stage 1 and stage 2. (C) Volcano-plots of differentially expressed genes in

455 stage 1 and stage 2. (D) Heatmap of differentially expressed genes in stage 1 and stage 2. The

456 numbers ranging from -2 to 2 represented the expression level from low to high based Z-score

457 method.

458

459 **Figure 3.** GO function enrichment analysis of differentially expressed genes. (A) Biological

460 progress. (B) Molecular function. (C) Cellular component. Fisher's exact test, adjusted P-value

461 was performed by the Benjamini-Yekutieli method (FDR < 0.05).

462

463 **Figure 4.** KEGG enrichment analysis of differentially expressed genes of stage 1 vs stage 2. The

464 abscissa indicates the degree of significant enrichment.

465

466 **Figure 5.** Analysis of leaf metabolites in different periods. (A) Differential metabolite analysis on

467 the basis of principal component analysis (PCA) between stage 1 and stage 2. (B) OPLS-DA model

468 plots for the comparison group stage 1 vs stage 2. (C) Differential metabolite heatmap of stage 1

469 vs stage 2, metabolites ID can be found in Table S2. (D) Analysis of common KEGG metabolic

470 pathways between stage 1 and stage 2.

471

472 **Figure 6.** Association analysis of metabolomics and transcriptomics data. (A) Divergent gene and

473 metabolite loading map of stage 1 and stage 2. Each point in the figure represents a gene or a

474   metabolite. The abscissa is the first-dimensional coordinate of the joint part, and the ordinate is

475   the second-dimensional coordinate of the joint part. The greater the absolute value of the element

476   in the coordinate, the greater the correlation between this element and another group. (B) Network

477   diagram of the correlation between differential gene expression and differential metabolite

478   abundance, top 250 pairs of genes and metabolites (with the absolute pearson correlation > 0.5)

479   were applied for metabolite-transcript network analysis.

480

481   **Figure 7.** Expression level of anthocyanin and synthesis pathway-related genes. (A)

482   Transcriptome data of anthocyanin synthesis pathway-related genes. (B) qRT-PCR results of

483   anthocyanin synthesis pathway-related genes in different stages. Error bar represents the mean ±

484   SD of three independent biological replicates. (C) Transcriptome data of anthocyanidin synthesis

485   pathway-related genes *BZ1* and *UGT79B1*. (D) qRT-PCR results of *BZ1* and *UGT79B1* in two

486   stages. Error bar represents the mean ± SD of three independent biological replicates.

487

488   **Figure S1.** Integrity evaluation of *Fraxinus angustifolia* transcriptome data in stage 1 and stage 2.

489   **Figure S2.** Pearson correlation coefficient analysis based on the expression level of stage 1 and

490   stage 2.

491   **Figure S3.** OPLSDA loadings plot of *Fraxinus angustifolia* metabolites in stage 1 and stage 2.

492   **Figure S4.** Anthocyanin biosynthesis diagrams based on differentially expressed genes in stage 1

493   and stage 2.

494

495   **Table S1.** Statistics of transcriptome clean data.

496   **Table S2.** Name, type and expression of metabolites in stage 1 and stage 2, values of stage 1 and

497   stage 2 represent expression data of metabolites.

498

499 **References**

500 **Allan AC, Hellens RP, and Laing WA. 2008.** MYB transcription factors that colour our fruit.

501 *Trends in Plant Science* **13:**99-102 DOI 10.1016/j.tplants.2007.11.012

502 **Belwal T, Singh G, Jeandet P, Pandey A, Giri L, Ramola S, Bhatt ID, Venskutonis PR,**

503 **Georgiev MI, Clement C, and Luo Z. 2020.** Anthocyanins, multi-functional natural products of

504 industrial relevance: Recent biotechnological advances. *Biotechnology Advances* **43:**107600 DOI

505 10.1016/j.biotechadv.2020.107600

506 **Bouhaddani SE, Uh HW, Jongbloed G, Hayward C, Klaric L, Kielbasa SM, and Houwing-**

507 **Duistermaat J. 2018.** Integrating omics datasets with the OmicsPLS package. *BMC*

508 *Bioinformatics* **19:**371 DOI 10.1186/s12859-018-2371-3

509 **Brown J, Pirrung M, and McCue LA. 2017.** FQC Dashboard: integrates FastQC results into a

510 web-based, interactive, and extensible FASTQ quality control tool. *Bioinformatics* **33:**3137-3139

511 DOI 10.1093/bioinformatics/btx373

512 **Butelli E, Titta L, Giorgio M, Mock HP, Matros A, Peterek S, Schijlen EG, Hall RD, Bovy**

513 **AG, Luo J, and Martin C. 2008.** Enrichment of tomato fruit with health-promoting anthocyanins

514 by expression of select transcription factors. *Nature Biotechnology* **26:**1301-1308 DOI

515 10.1038/nbt.1506

516 **Cheng J, Liao L, Zhou H, Gu C, Wang L, and Han Y. 2015.** A small indel mutation in an

517 anthocyanin transporter causes variegated colouration of peach flowers. *Journal of Experimental*

518 *Botany* **66** DOI 10.1093/jxb/erv419

519 **Chiu LW, Zhou X, Burke S, Wu X, Prior RL, and Li L. 2010.** The purple cauliflower arises

520 from activation of a MYB transcription factor. *Plant Physiology* **154:**1470-1480

521 10.1104/pp.110.164160

522 **Conesa A, and Gotz S. 2008.** Blast2GO: A comprehensive suite for functional analysis in plant

523 genomics. *International Journal of Plant Genomics* **2008:**619832 DOI 10.1155/2008/619832

524 **Das PK, Geul B, Choi SB, Yoo SD, and Park YI. 2011.** Photosynthesis-dependent anthocyanin

525 pigmentation in Arabidopsis. *Plant signaling & behavior* **6:**23-25 DOI 10.4161/psb.6.1.14082

526 **Guo X, Fu X, Li X, and Tang D. 2022.** Effect of flavonoid dynamic changes on flower coloration

527 of *Tulipa gesneiana* 'Queen of Night' during clower development. *Horticulturae* **8**, 510 DOI

528 10.3390/horticulturae8060510

529 **Hashimoto H, Uragami C, and Cogdell RJ. 2016.** Carotenoids and Photosynthesis. *Subcellular*

530 *Biochemistry* **79:**111-139 DOI 10.1007/978-3-319-39126-7_4

531 **Jin J, Tian F, Yang DC, Meng YQ, Kong L, Luo J, and Gao G. 2017.** PlantTFDB 4.0: toward

532 a central hub for transcription factors and regulatory interactions in plants. *Nucleic Acids Research*

533 **45:** D1040-D1045 DOI 10.1093/nar/gkw982

534 **Kong JM, Chia LS, Goh NK, Chia TF, and Brouillard R. 2003.** Analysis and biological

535 activities of anthocyanins. *Phytochemistry* **64:**923-933 DOI 10.1016/s0031-9422(03)00438-2

536 **Li Y, He N, Hou J, Xu L, Liu C, Zhang J, Wang Q, Zhang X, and Wu X. 2018.** Factors

537 influencing leaf chlorophyll content in natural forests at the biome scale. *Frontiers in Ecology and*

538 *Evolution* **6:**64 DOI 10.3389/fevo.2018.00064

539 **Liu W, Feng Y, Yu S, Fan Z, Li X, Li J, and Yin H. 2021.** The flavonoid biosynthesis network

540 in plants. *International Journal Of Molecular Sciences* **22:**12824 DOI 10.3390/ijms222312824

541 **Love MI, Huber W, and Anders S. 2014.** Moderated estimation of fold change and dispersion

542 for RNA-seq data with DESeq2. *Genome Biology* **15:**550 DOI 10.1186/s13059-014-0550-8

543 **Luiza Koop B, Nascimento da Silva M, Diniz da Silva F, Thayres Dos Santos Lima K, Santos**

544 **Soares L, Jose de Andrade C, Ayala Valencia G, and Rodrigues Monteiro A. 2022.**

545 Flavonoids, anthocyanins, betalains, curcumin, and carotenoids: Sources, classification and

546 enhanced stabilization by encapsulation and adsorption. *Food Research International* **153:**110929

547 DOI 10.1016/j.foodres.2021.110929

548 **Luo J, Shi Q, Niu L, and Zhang Y. 2017.** Transcriptomic analysis of leaf in tree peony reveals

549 differentially expressed pigments genes. *Molecules* **22** DOI 10.3390/molecules22020324

550 **Manni M, Berkeley MR, Seppey M, and Zdobnov EM. 2021.** BUSCO: Assessing Genomic

551 Data Quality and Beyond. *Current Protocol* **1:**e323 DOI 10.1002/cpz1.323

552 **Manzanera JA, and Martinez-Chacon MF. 2007.** Ecophysiological competence of Populus alba

553 L., *Fraxinus angustifolia* Vahl., and *Crataegus monogyna* Jacq. used in plantations for the

554 recovery of riparian vegetation. *Environment Management* **40:**902-912 DOI 10.1007/s00267-007-

555 9016-z

556 **Meng X, Li G, Gu L, Sun Y, Li Z, Liu J, Wu X, Dong T, and Zhu M. 2020.** Comparative

557 metabolomic and transcriptome analysis reveal distinct flavonoid biosynthesis regulation between

558 petals of white and purple *Phalaenopsis amabilis*. *Journal of Plant Growth Regulation* **39:**823-

559 840 DOI 10.1007/s00344-019-10025-y

560 **Mishio T, Takeda K, and Iwashina T. 2015.** Anthocyanins and other flavonoids as flower

561 pigments from eleven *Centaurea* species. *Nature Product Communacation* **10:**447-450 DOI

562 10.1177/1934578X15010003

563 **Ohno S, Hosokawa M, Hoshino A, Kitamura Y, Morita Y, Park K-I, Nakashima A, Deguchi**

564 **A, Tatsuzawa F, Doi M, Iida S, and Yazawa S. 2011.** A bHLH transcription factor, DvIVS, is

565 involved in regulation of anthocyanin synthesis in dahlia (*Dahlia variabilis*). *Journal of*

566 *Experimental Botany* **62:**5105-5116 DOI 10.1093/jxb/err216

567 **Özbayram AK, and Çiçek E. 2018.** Thinning experiments in narrow-leaved ash (*Fraxinus*

568 *angustifolia* Vahl.) plantations: 10-year results. *New Forests* **49:**585-598 DOI 10.1007/s11056-

569 018-9642-8

570 **Ranjan S, Singh R, Singh M, Pathre UV, and Shirke PA. 2014.** Characterizing photoinhibition

571 and photosynthesis in juvenile-red versus mature-green leaves of *Jatropha curcas* L. *Plant*

572 *Physiology and Biochemistry* **79:**48-59 DOI 10.1016/j.plaphy.2014.03.007

573 **Ravaglia D, Espley RV, Henry-Kirk RA, Andreotti C, Ziosi V, Hellens RP, Costa G, and**

574 **Allan AC. 2013.** Transcriptional regulation of flavonoid biosynthesis in nectarine (*Prunus*

575 *persica*) by a set of R2R3 MYB transcription factors. *BMC Plant Biology* **13:**68 DOI

576 10.1186/1471-2229-13-68

577 **Rizzato G, Scalabrin E, Radaelli M, Capodaglio G, and Piccolo O. 2017.** A new exploration

578 of licorice metabolome. *Food Chemistry* **221:**959-968 DOI 10.1016/j.foodchem.2016.11.068

579 **Santos-Buelga C, Mateus N, and De Freitas V. 2014.** Anthocyanins, plant pigments and beyond.

Journal of Agricultural and Food Chemistry **62:**6879-6884 DOI 10.1021/jf501950s

Sarfraz I, Rasul A, Jabeen F, Younis T, Zahoor MK, Arshad M, and Ali M. 2017. Fraxinus: a plant with versatile pharmacological and biological activities. *Evidence-based Complementary and Alternative Medicine* **2017:**4269868 DOI 10.1155/2017/4269868

Schauer N, and Fernie AR. 2006. Plant metabolomics: towards biological function and mechanism. *Trends in Plant Science* **11:**508-516 DOI 10.1016/j.tplants.2006.08.007

Sewe SO, Silva G, Sicat P, Seal SE, and Visendi P. 2022. Trimming and validation of illumina short reads using trimmomatic, trinity assembly, and assessment of RNA-Seq data. *Methods Molecular Biology* **2443:**211-232 DOI 10.1007/978-1-0716-2067-0_11

Sharma A, Mazumdar B, and Keshav A. 2021. Valorization of unsalable *Amaranthus tricolour* leaves by microwave-assisted extraction of betacyanin and betaxanthin. *Biomass Conversion and Biorefinery* DOI 10.1007/s13399-020-01267-y

Song YH, Ito S, and Imaizumi T. 2013. Flowering time regulation: photoperiod- and temperature-sensing in leaves. *Trends in Plant Science* **18:**575-583 10.1016/j.tplants.2013.05.003

Sork VL, Davis FW, Westfall R, Flint A, Ikegami M, Wang H, and Grivet D. 2010. Gene movement and genetic association with regional climate gradients in California valley oak (*Quercus lobata* Nee) in the face of climate change. *Molecular Ecology* **19:**3806-3823 DOI 10.1111/j.1365-294X.2010.04726.x

Sun C, Wang C, Zhang W, Liu S, Wang W, Yu X, Song T, Yu M, Yu W, and Qu S. 2021. The R2R3-type MYB transcription factor MdMYB90-like is responsible for the enhanced skin color of an apple bud sport mutant. *Horticulture Research* **8:**156 DOI 10.1038/s41438-021-00590-3

Tanaka Y, Sasaki N, and Ohmiya A. 2008. Biosynthesis of plant pigments: anthocyanins, betalains and carotenoids. *Plant J* **54:**733-749 DOI 10.1111/j.1365-313X.2008.03447.x

Tian T, Liu Y, Yan H, You Q, Yi X, Du Z, Xu W, and Su Z. 2017. AgriGO v2.0: a GO analysis toolkit for the agricultural community, 2017 update. *Nucleic Acids Research*, **45**, W122-W129 DOI 10.1093/nar/gkx382

607 **Wang L, Tang W, Hu Y, Zhang Y, Sun J, Guo X, Lu H, Yang Y, Fang C, Niu X, Yue J, Fei**

608 **Z, and Liu Y. 2019.** A MYB/bHLH complex regulates tissue-specific anthocyanin biosynthesis

609 in the inner pericarp of red-centered kiwifruit *Actinidia chinensis* cv. Hongyang. *The Plant Journal*

610 **99:**359-378 DOI 10.1111/tpj.14330

611 **Wang X, and Kadarmideen HN. 2020.** Metabolite genome-wide association study (mGWAS)

612 and gene-metabolite interaction network analysis reveal potential biomarkers for feed efficiency

613 in pigs. *Metabolites* **10:**201 DOI 10.3390/metabo10050201

614 **Wang ZX, Yu YF, Chen L, Qin HY, Liu YX, Ai J, Zhao Y, Yang YM, Li XY, Wang GF, Sun**

615 **D, Wang CW, and Fan ST. 2016.** Advances in leaf pigment composition, structure and

616 photosynthetic characteristics of colored-leaf plants. *Plant Physiology Journal* **52:**1-7 DOI

617 10.13592/j.cnki.ppj.2015.0490

618 **Zhang DW, Yuan S, Xu F, Zhu F, Yuan M, Ye HX, Guo HQ, Lv X, Yin Y, and Lin HH. 2016.**

619 Light intensity affects chlorophyll synthesis during greening process by metabolite signal from

620 mitochondrial alternative oxidase in Arabidopsis. *Plant Cell & Environment* **39:**12-25 DOI

621 10.1111/pce.12438

622 **Zhang Q, Liu M, and Ruan J. 2017.** Metabolomics analysis reveals the metabolic and functional

623 roles of flavonoids in light-sensitive tea leaves. *BMC Plant Biology* **17:**64 DOI 10.1186/s12870-

624 017-1012-8

625 **Zhang Q, Zhai J, Shao L, Lin W, and Peng C. 2019.** Accumulation of anthocyanins: an

626 adaptation strategy of *Mikania micrantha* to low temperature in winter. *Frontiers in Plant Science*

627 **10:**1049 DOI 10.3389/fpls.2019.01049

628 **Zhao M-H, Li X, Zhang X-X, Zhang H, and Zhao X-Y. 2020.** Mutation mechanism of leaf color

629 in plants: a review. *Forests* **11:**851 DOI 10.3390/f11080851

630 **Zhao X, Zhang Y, Long T, Wang S, and Yang J. 2022.** Regulation mechanism of plant pigments

631 biosynthesis: anthocyanins, carotenoids, and betalains. *Metabolites* **12** DOI

632 10.3390/metabo12090871

633 **Zhao Y, and Kong L. 2021.** KOBAS-i: intelligent prioritization and exploratory visualization of

634   biological functions for gene enrichment analysis. *Nucleic Acids Research*, **49**, W317-W325 DOI

635   10.1093/nar/gkab447

636   **Zhou F, Peng J, Zhao Y, Huang W, Jiang Y, Li M, Wu X, and Lu B. 2017.** Varietal

637   classification and antioxidant activity prediction of Osmanthus fragrans Lour. flowers using

638   UPLC-PDA/QTOF-MS   and   multivariable   analysis.   *Food   Chemistry*   **217:**490-497   DOI

639   10.1016/j.foodchem.2016.08.125

640

Figure 1

Figure 1

Figure 1. Statistical analysis of transcriptome data. (A) Leaf states at stage 1 and stage 2. (B) Length distribution of Unigene in transcriptome assembly. (C) Venn diagram of Unigene annotation in the Nr, KEGG, KOG, and SwissProt databases.
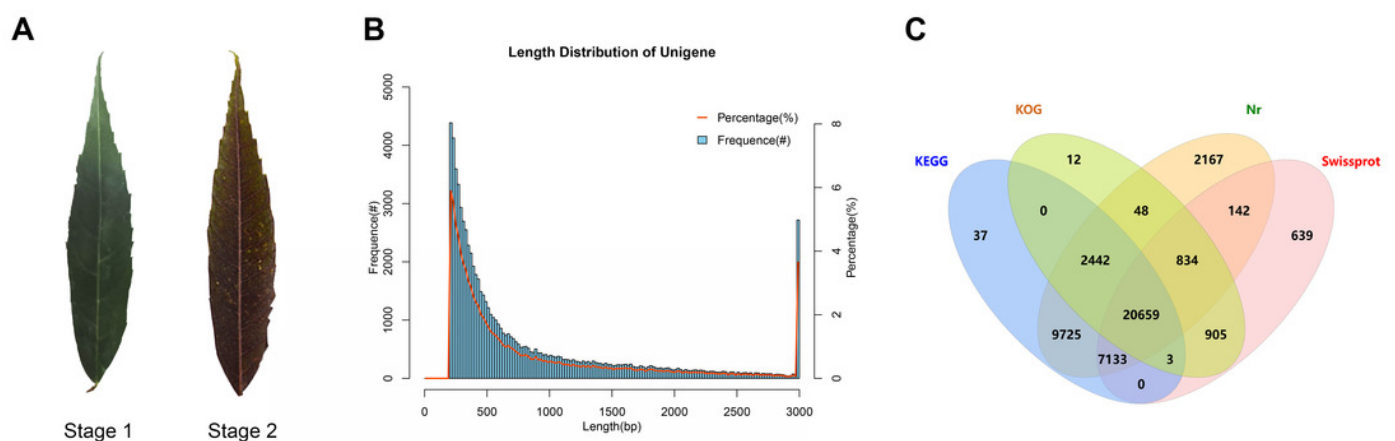
Figure 2

Figure 2

Figure 2. Expression analysis of Unigenes in stage 1 and stage 2. (A) Expression level analysis of different biological replicates in stage 1 and stage 2. (B) Principal component analysis (PCA) of expression datasets in stage 1 and stage 2. (C) Volcano-plots of differentially expressed genes in stage 1 and stage 2. (D) Heatmap of differentially expressed genes in stage 1 and stage 2. The numbers ranging from -2 to 2 represented the expression level from low to high based Z-score method.

A

log10(fpkm) violin plot for samples Stage1-1, Stage1-2, Stage1-3, Stage2-1, Stage2-2, Stage2-3

B

PCA

PC2(17.7%) vs PC1(73.1%)

group
● Stage1
▲ Stage2

B

Stage1-vs-Stage2

-log10(FDR) vs log2(fc)

● up
● nosig
● down

C

Heatmap of samples Stage2-2, Stage2-1, Stage2-3, Stage1-2, Stage1-1, Stage1-3
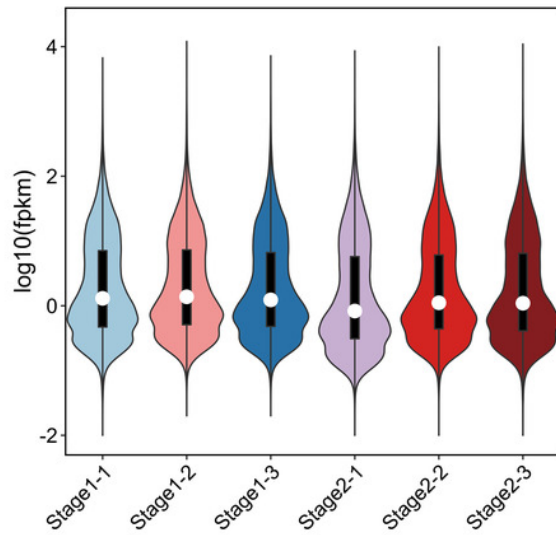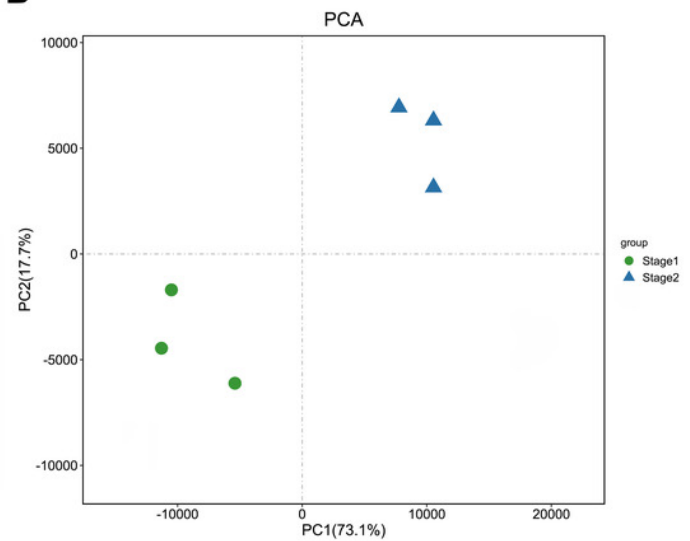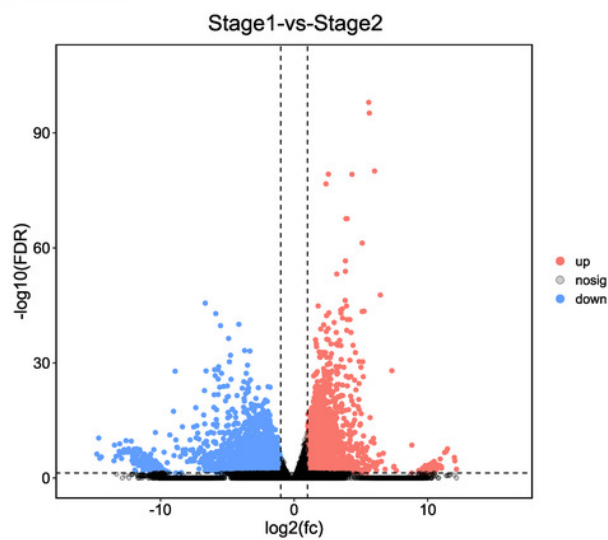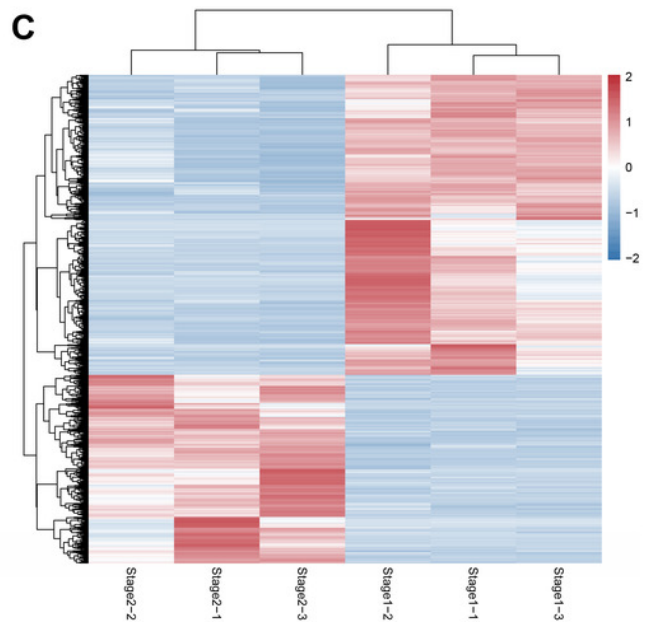
Figure 3

Figure 3

Figure 3. GO function enrichment analysis of differentially expressed genes. (A) Biological progress. (B) Molecular function. (C) Cellular component. Fisher's exact test, adjusted P-value was performed by the Benjamini-Yekutieli method (FDR < 0.05).
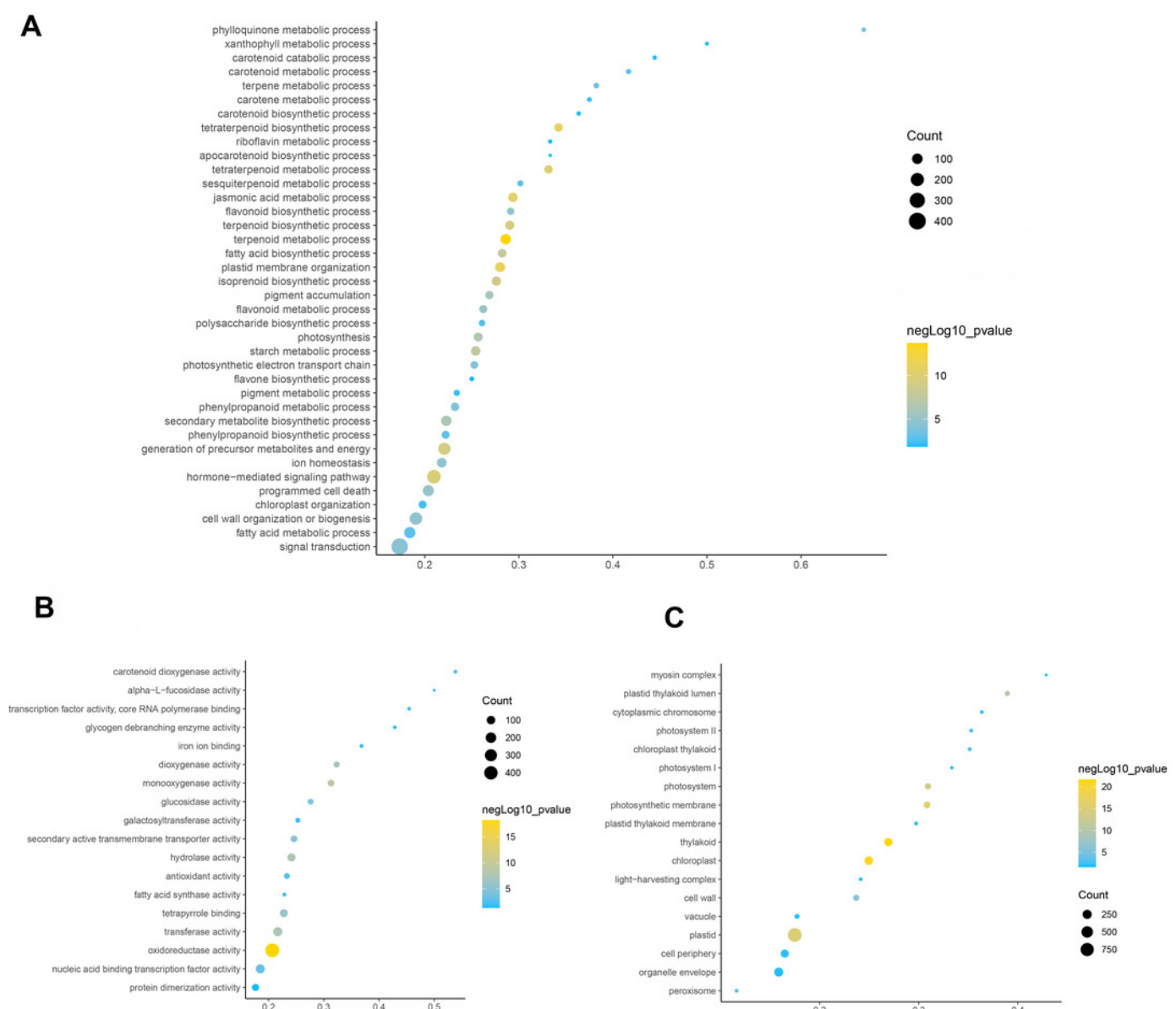
Figure 4

Figure 4

Figure 4. KEGG enrichment analysis of differentially expressed genes of stage 1 vs stage 2. The abscissa indicates the degree of significant enrichment.
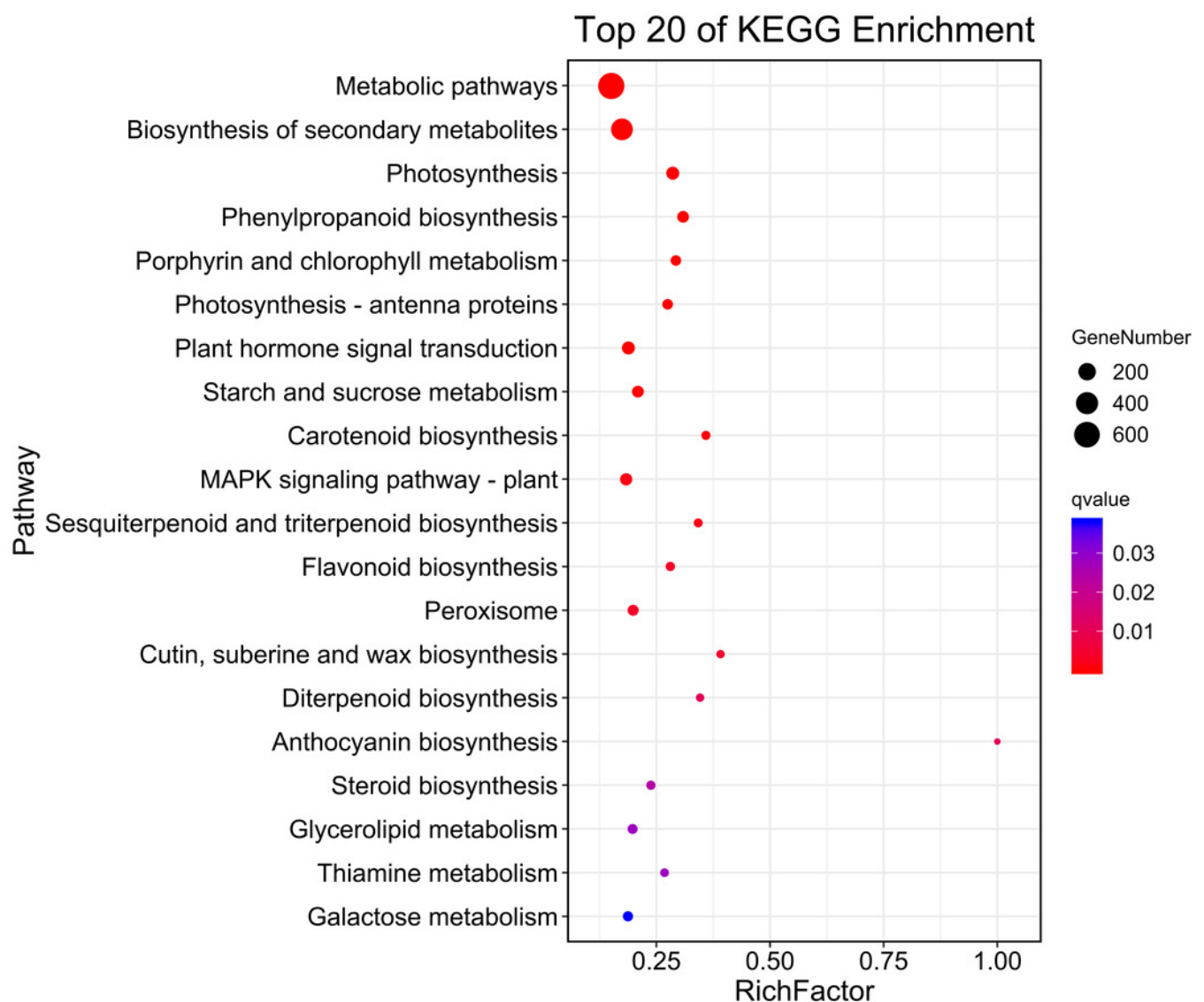
Figure 5

Figure 5

Figure 5. Analysis of leaf metabolites in different periods. (A) Differential metabolite analysis on the basis of principal component analysis (PCA) between stage 1 and stage 2. (B) OPLS-DA model plots for the comparison group stage 1 vs stage 2. (C) Differential metabolite heatmap of stage 1 vs stage 2, metabolites ID can be found in Table S2. (D) Analysis of common KEGG metabolic pathways between stage 1 and stage 2.
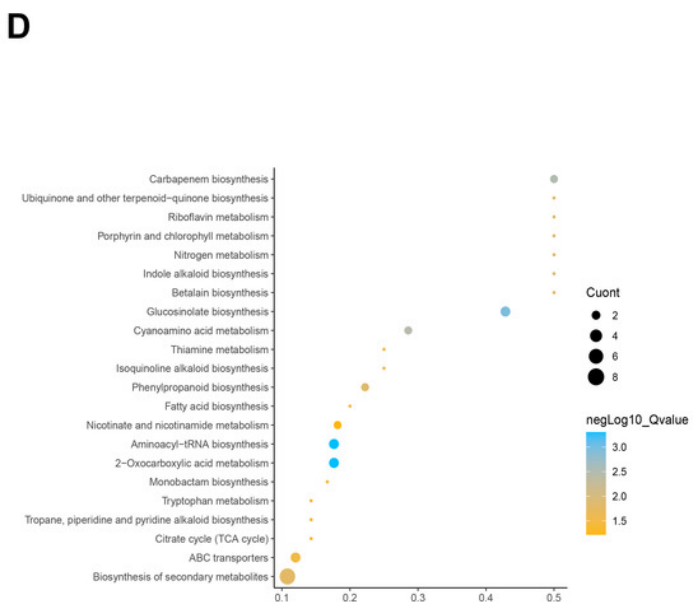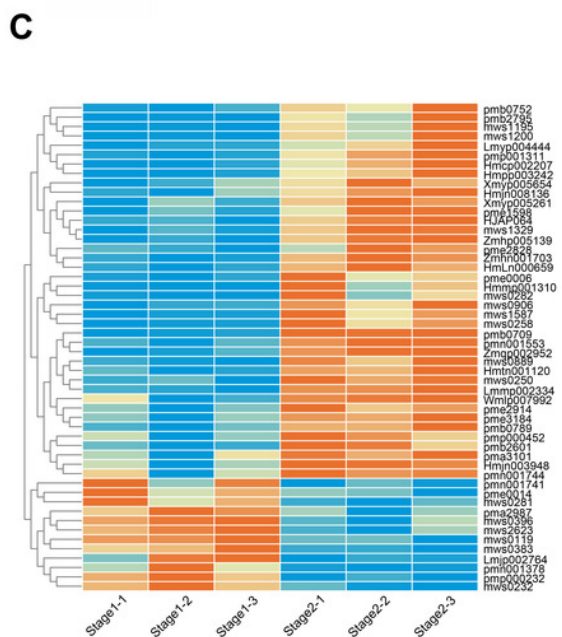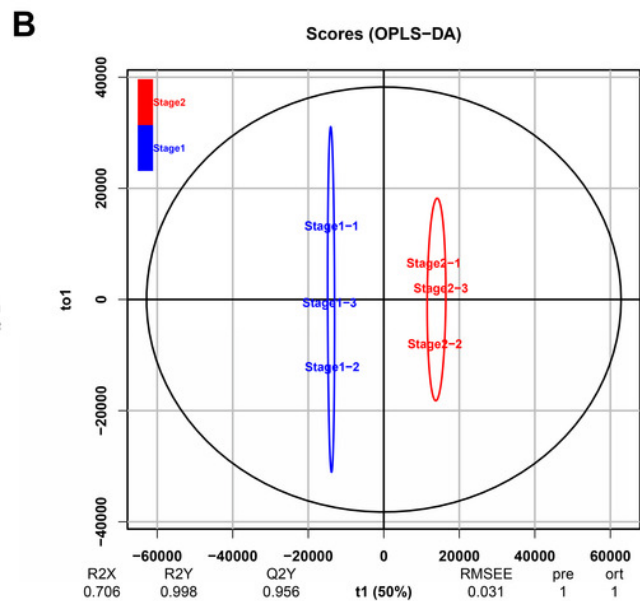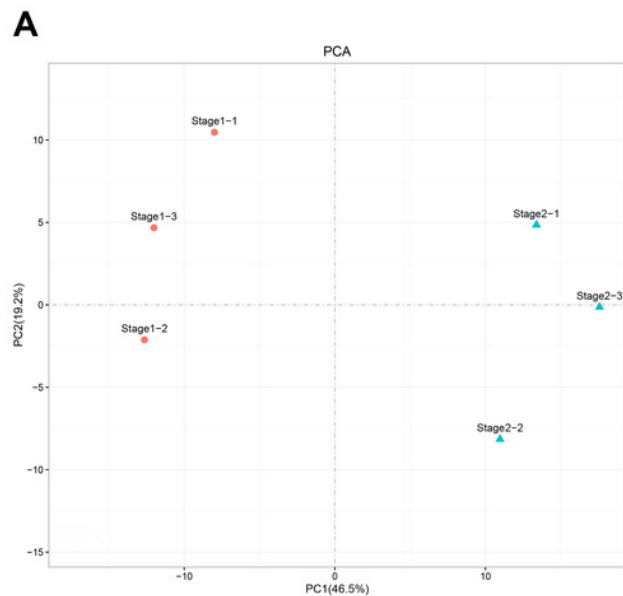
A

PCA

B

Scores (OPLS-DA)

C

D

Figure 6

Figure 6

Figure 6. Association analysis of metabolomics and transcriptomics data. (A) Divergent gene and metabolite loading map of stage 1 and stage 2. (B) Network diagram of the correlation between differential gene expression and differential metabolite abundance.
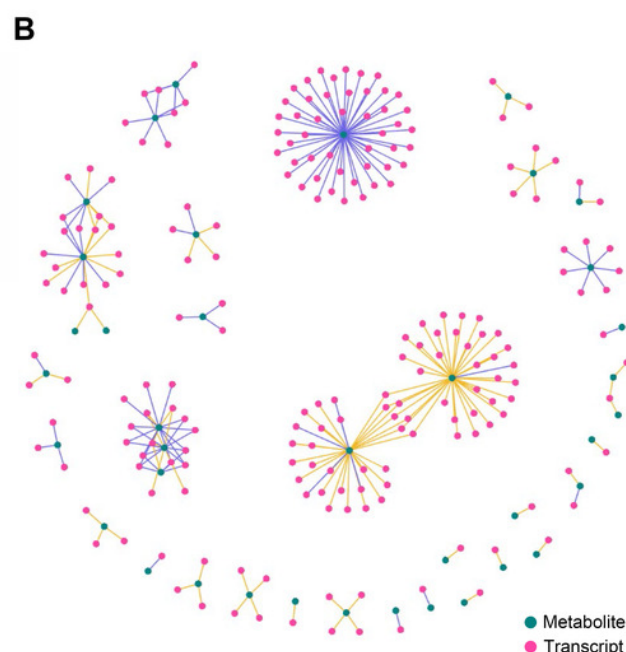
Figure 7

Figure 7

Figure 7. Expression level of anthocyanin and synthesis pathway-related genes. (A) Transcriptome data of anthocyanin synthesis pathway-related genes. (B) qRT-PCR results of anthocyanin synthesis pathway-related genes in different stages. Error bar represents the mean ± SD of three independent biological replicates. (C) Transcriptome data of anthocyanidin synthesis pathway-related genes *BZ1* and *UGT79B1*. (D) qRT-PCR results of *BZ1* and *UGT79B1* in two stages. Error bar represents the mean ± SD of three independent biological replicates.